

1        **Use of ferric impregnated volcanic ash for arsenate(V) adsorption**  
2        **from contaminated water with various mineralization degrees**

3                Rongzhi Chen<sup>a</sup>, Zhenya Zhang<sup>a,\*</sup>, Yingnan Yang<sup>a</sup>, Zhongfang Lei<sup>b</sup>, Norio Sugiura<sup>a</sup>.

4        <sup>a</sup> Graduate School of Life and Environmental Sciences, University of Tsukuba, Tsukuba 305-8572,  
5        Japan

6        <sup>b</sup> Department of Environmental Science and Engineering, Fudan University, Shanghai 200433, China

7        **Abstract**

8                Ferric impregnated volcanic ash (FVA) which consisted mainly of different  
9        forms iron and aluminum oxide minerals was developed for arsenate (V) removal  
10       from the aqueous medium. The adsorption experiments were conducted in both DI  
11       water samples and the actual water (*Lake Kasumigaura*, Japan) to investigate the  
12       effects of solution mineralization degree on the As(V) removal. Kinetic and  
13       equilibrium studies conducted in actual water revealed that the mineralization of  
14       water greatly elevated the As(V) adsorption on FVA. The experiment performed in DI  
15       water indicated that the existence of multivalence metallic cations significantly  
16       enhanced the As(V) adsorption ability, whereas competing anions such as fluoride and  
17       phosphate greatly decreased the As(V) adsorption. It is suggested that FVA is a  
18       cost-effective adsorbent for As(V) removal in low-level phosphate and fluoride  
19       solution. It was important to conduct the batch experiment using the actual water to  
20       investigate the arsenic removal on adsorbents.

21                **Keywords:** Arsenate (V) adsorption, Actual water, Water mineralization, Ferric  
22       impregnated volcanic ash, Langmuir isotherm.

23        

---

\*Correspondence: Zhenya Zhang, Graduate School of Life and Environmental Sciences, University of  
24        Tsukuba, 1-1-1, Tennodai, Tsukuba, Ibaraki 305-8572, Japan.

25        Tel: 81-29-8534712

26        Fax: 81-29-8537496

1 E-mail: crz0718@gmail.com

## 2 **1. Introduction**

3 Arsenate in water is a widespread toxic contaminant which might cause many  
4 chronic and carcinogenic public health problems, such as cancer and skin diseases [1].  
5 It was reported that over 70 countries were suffering from natural arsenic pollution,  
6 posing a serious health hazard to an estimated 150 million people world-wide [2].  
7 Among them, more than 70% populations lived in Asia, especially in South and  
8 South-east of Bangladesh, China, and India [3, 4]. Maximum Contaminant Level  
9 (MCL) of arsenic in drinking water, suggested by World Health Organization (WHO)  
10 in 1996, is 10 µg /L [5]. This standard has been adopted by European Union and USA  
11 in 1998 and 2001 [6, 7]. However, the standard is fivefold higher than that of WHO in  
12 China, India and some other developing countries where a high risk of arsenic  
13 poisoning exists [2]. There is urgent need for develop a cost- effective technology for  
14 arsenic removal for aqueous medium.

15 Several methods are available for arsenic removal from aqueous medium,  
16 including adsorption, ion exchange, lime softening, reverse osmosis, coagulation, and  
17 precipitation [8 -10]. Given its advantages and limitations, the adsorption has been  
18 recognized as a favorable technology which has the advantages of convenient process,  
19 high removal efficiency, regeneration potential and sludge free. Many former studies  
20 had investigated agricultural products, industrial by-products/wastes, soils and clay  
21 minerals as promising adsorbents for arsenic, such as, red mud or fly ash [11, 12].  
22 They had built a win-win system for waste utilization and disposal of environmental  
23 accumulated hazard due to their high alkalinity and large amount.

24 Volcanic ash (VA), as a similar environmental load to red mud and fly ash, is one  
25 of the major hazards from volcanic eruptions. Significant accumulations of volcanic

1 ash ashfall can lead to the immediate destruction of most of the local ecosystem, as  
2 well as damage on man-made structures, such as, severely damage jet engines, abrade  
3 surfaces, clog air filters, obstruct surface transportation, and shut down major airports  
4 [13]. Volcanic ash mainly consisted of different forms of iron and aluminum oxide  
5 minerals, which were contribute to arsenic adsorption [11, 12]. In this study, volcanic  
6 ash was first used for arsenic removal from aqueous medium. We loaded iron  
7 (hydro)oxides on the surface of volcanic ash through ferric impregnation and  
8 moderate temperature coating treatments, in order to enhance the arsenic affinity to  
9 adsorbent.

10 Arsenic sorption was commonly studied in terms of the effects of adsorbent  
11 (dosage and particle size) and solution properties (initial concentration, pH, and  
12 temperature). However, less attention was paid to the solution mineralization, which  
13 was believed it also showed great influence on the arsenic adsorption [14,16-19]. Guo  
14 et al. [17] reported the presence of phosphate greatly impeded the adsorption of  
15 arsenate, and Sun et al. [18] showed that the presence of high-level nitrate anion can  
16 accelerate arsenate removal while phosphate provides a competitive effect. Xu et al.  
17 [14] and Roberts et al. [19] also studied effects of anions on As removal. But there are  
18 comparatively few studies published on the effect of cations on As removal. Besides,  
19 the batch experiments are usually carried out with deionized water and influence of  
20 water chemistry is not well studied. Given the fact that degree of water mineralization  
21 varies in most contaminated aqueous systems, it is important to investigate arsenic  
22 removal based on actual waters instead of deionized water.

23 The purpose of present study was to develop and investigate ferric impregnated  
24 volcanic ash (FVA) as an alternate As(V) adsorbent. The effects of mineralization  
25 degree (ion competition and ionic strength) on the arsenic removal efficiency were

1 systematically researched. Kinetic and equilibrium studies of arsenic removal in  
2 actual waters by FVA were discussed.

## 3 **2. Materials and methods**

### 4 *2.1. Materials*

5 Volcanic ash was provided by Makino Store, Kiyosu, Japan. The chemical  
6 composition was analyzed through the semi-quantitative elemental analysis and  
7 element mapping by energy dispersive X-ray spectrometry (EDX). The result was  
8 listed in Table 1 and it shows that volcanic ash is primarily a mixture of Si, Fe and Al  
9 oxides. 5g samples were crushed and sieved to obtain fractions of particle size smaller  
10 than 150 mesh, and then impregnated with ferric solution (FeCl<sub>3</sub>, 20g/l) in a water  
11 thermostat (50 °C). The impregnated samples were calcined in a muffle furnace at  
12 300°C for 1 h, and the cooling samples were re-sieved through a 150-mesh screen for  
13 future study.

14 Table 1  
15 Chemical analysis of VA and FVA

Composition ( wt %)	SiO <sub>2</sub>	Al <sub>2</sub> O <sub>3</sub>	Fe <sub>2</sub> O <sub>3</sub>	MgO	CaO	MnO	pH <sub>zpc</sub>
VA	51.30	38.05	7.67	1.94	0.78	0.26	6.9 ± 0.5
FVA	48.40	36.53	12.75	1.62	0.46	0.24	5.5 ± 0.5

16  
17 As(V) stock solutions (1000mg/L) were prepared by dissolving sodium hydrogen  
18 arsenate (Na<sub>2</sub>HAsO<sub>4</sub>·7H<sub>2</sub>O, Wako Pure Chemical Industries) in deionized water (DI)  
19 of pH 6.9. The coexisting ions were provided by analytical grade chemicals (KCl,  
20 CaCl<sub>2</sub>, FeCl<sub>3</sub>, NaCl, NaF, NaNO<sub>3</sub>, Na<sub>2</sub>SO<sub>4</sub>, and Na<sub>3</sub>PO<sub>4</sub>, Wako Pure Chemical  
21 Industries), and the solution ionic strength was adjusted to 0.001, 0.01 and 0.1 M with  
22 NaCl, which were used to produce various water mineralization degrees.

23 Furthermore, two actual water samples, named W1 to W2, with different  
24 compositions have been selected in order to test the influence of water mineralization  
25 on As(V) removal in real water solution. W1 is a tap water sample from our

1 laboratory; W2 is a surface layer water sample taken from *Lake Kasumigaura*, the  
 2 second largest lake in Japan. The chemical compositions information was shown in  
 3 Table 2. In all the samples the arsenic concentration was below the detection limits  
 4 ( $1\mu\text{g/L}$ ) determined by an inductively coupled plasma atomic emission spectrometer.

5 Table 2  
 6 Chemical compositions and characteristics of the water samples

Water sample		W0	W1	W2
Composition		Deionised water	Tap water	Lake water
Sodium	$\text{mg L}^{-1}$	0.6	26.9	43.4
Magnesium	$\text{mg L}^{-1}$	<0.1	6.7	6.2
Calcium	$\text{mg L}^{-1}$	0.4	22.0	28.7
Potassium	$\text{mg L}^{-1}$	0.3	6.7	15.1
Fluoride	$\text{mg L}^{-1}$	0.5	0.2	0.2
Sulfate	$\text{mg L}^{-1}$	0.2	22.8	35.4
Chloride	$\text{mg L}^{-1}$	0.2	50.1	119.2
Nitrate	$\text{mg L}^{-1}$	<0.1	2.4	8.6
Phosphate	$\text{mg L}^{-1}$	<0.1	<0.1	1.0
pH	pH unit	6.72	7.19	7.87

## 7 2.2. Methods

### 8 2.2.1. Analysis methods

9 The prepared FVA was analyzed in order to determine its physicochemical and  
 10 mineralogical properties. Specific surface area and pore size distributions were  
 11 determined by a gravimetric Brunauer–Emmett–Teller (BET) specific surface analysis  
 12 device (Coulter SA3100, US). The morphological features of FVA and VA were  
 13 analyzed by a scanning electron microscope (SEM, JSM-6700F, JEOL, Japan).  
 14 Mineralogical phase characterization was carried out using the quantitative X-ray  
 15 diffraction (XRD, RINT2200, Rigaku, Japan). The anions of water samples were  
 16 measured by an ion chromatography (IC7000, AS9-HC column, Yokogawa, Japan)  
 17 and major cations in water samples and As(V) concentrations were determined by an  
 18 inductively coupled plasma atomic emission spectrometer (ICP-AES, ICPS-7500,  
 19 Shimadzu, Japan). The point of zero charge ( $\text{pH}_{\text{pzc}}$ ) of FVA was estimated by using

1 batch equilibrium techniques described by Chutia et al. [20].

### 2 2.2.2. *Batch experiments*

3 Batch adsorptions contained two sets of experiments: kinetic and isotherm  
4 experiment. In order to know the static adsorption rate, kinetic experiments were  
5 carried out with the actual and DI water samples in a water thermostat ( $20 \pm 0.5^\circ\text{C}$ )  
6 without any agitations for 48h. 300 ml of synthetic As(V) solution (10 mg/L) was  
7 impregnated in the conical flask, with 10 g/L FVA. After centrifuging at 3000 rpm, the  
8 supernatant was filtered through a 0.45  $\mu\text{m}$  membrane filter and used to measure As(V)  
9 concentration by ICP-AES.

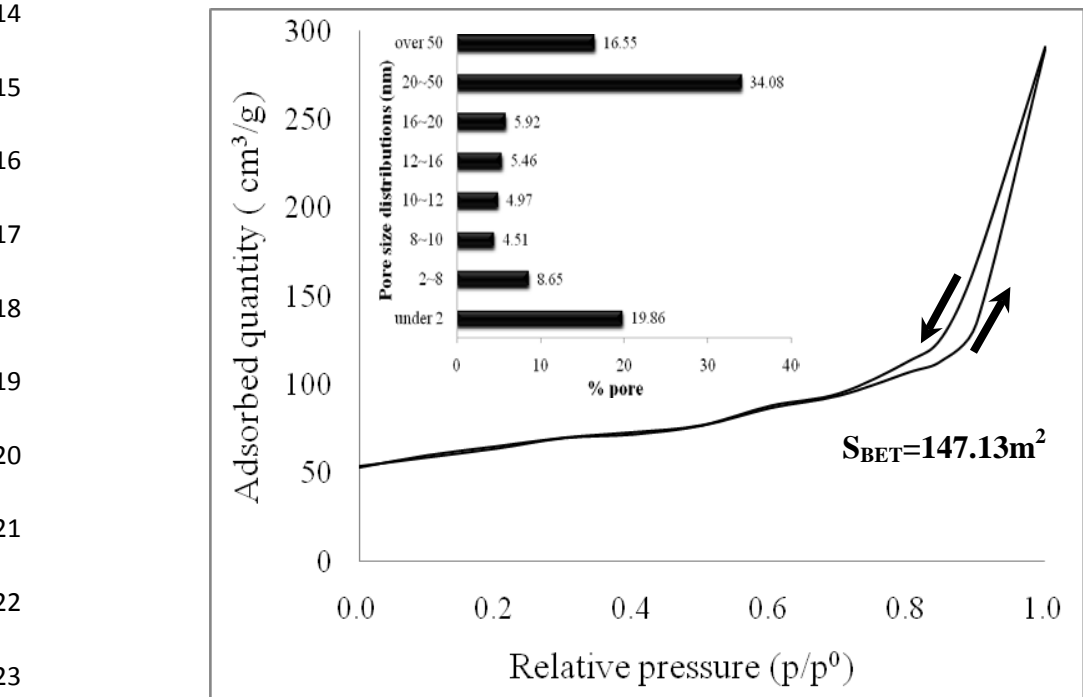
10 Isotherm experiments were performed to examine arsenic adsorption capacity on  
11 FVA in the water of different mineralization degrees, such as DI water (W0), tap  
12 water (W1) and lake water samples (W2). A 50 ml polyethylene centrifuge tube filled  
13 with 50 ml of As(V) (in concentrations ranging from 5 to 100mg/L) water samples  
14 and 10 g/L FVA were used to carry out the isotherm experiment. Considering that the  
15 plateau equilibrium need a long time, all isotherm tests were taken under an agitation  
16 speed of 200 rpm to shorten the equilibrium time.

17 Adsorption were conducted in both actual and DI water samples for  
18 investigating the relationship between the degree of water mineralization and As(V)  
19 removal. For the DI water, we adjusted the ionic strength of the solution or added  
20 other coexisting ions to simulate various mineralization degrees. The solution ionic  
21 strength was adjusted to 0.001, 0.01, and 0.1 M by adding the analytical grade NaCl.  
22 Coexisting ion tests were performed using As(V) solutions of 50 mg/L containing 5,  
23 and 50 mg/L of cations, including  $\text{K}^+$ ,  $\text{Ca}^{2+}$ , and  $\text{Fe}^{3+}$  (as  $\text{FeCl}_3$ ); and anions, including  
24  $\text{NO}_3^-$ ,  $\text{F}^-$ ,  $\text{SO}_4^{2-}$  and  $\text{PO}_4^{3-}$ . These ions represented univalent, bivalent and trivalent ions,  
25 respectively.

1 **3. Results and Discussion**

2 *3.1. Characterization of the prepared FVA*

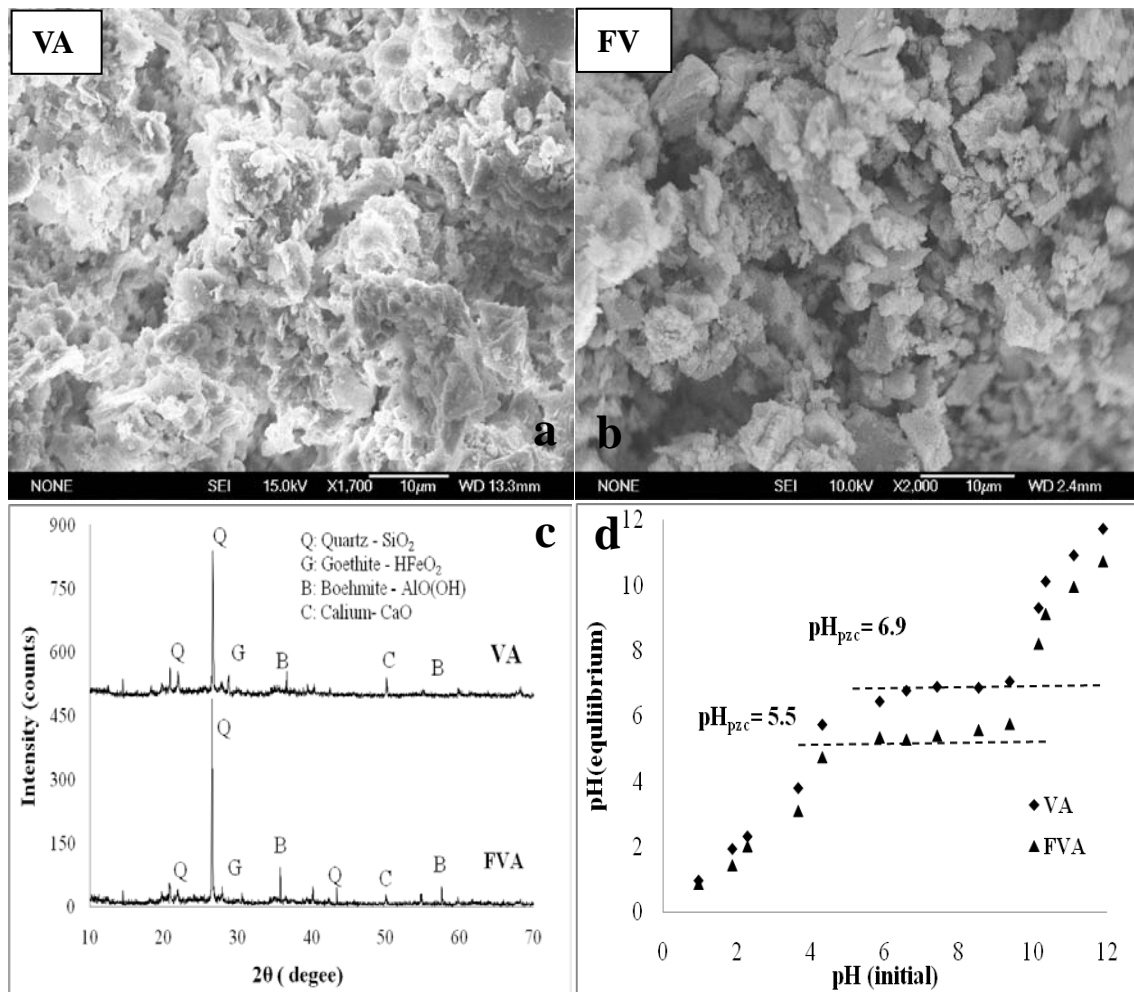
3 As shown in Fig. 1, the BET specific surface area of FVA was 147.13 sq.m/g.  
4 The BJH (Barrett–Joyner–Halenda) pore size distribution revealed that the observed  
5 pore sizes mostly varied between 2 and 50 nm (63.59%), according to the IUPAC  
6 classification which is typical for mesoporous materials. Fig. 2a and 2b are SEM  
7 images of FVA and VA in the initial Fe<sup>3+</sup> of 20g/L. The FVA initially forms a rough  
8 surface structure. Long-time (48h) solution erosion during impregnation appears to  
9 smooth the surface structure somewhat. It is also found that a few acicular and  
10 prismatic particles appeared on the surface after impregnation, which elevated the  
11 adsorption site. According to XRD analyses (Fig. 2c), the acicular and prismatic  
12 particles were identified as the boehmite (JCPDS 74-1895) and goethite (JCPDS  
13 81-0463).



14  
15  
16  
17  
18  
19  
20  
21  
22  
23  
24 Fig. 1. N<sub>2</sub> adsorption /desorption isotherm (77k) curve and pore size distributions of FVA (insert).

25 Local chemical composition of FVA is determined by SEM-EDX, together with

1 XRD pattern. As the results shown in Table 1, FVA mainly consist of the salic mineral  
 2 (aluminum oxides: 36.5%, silicon dioxide: 48.4%), comparing with VA, the iron  
 3 proportion increased to 12.75% due to the ferric impregnation. Fig. 2c shows the  
 4 XRD patterns of VA and FVA in initial As (V) of 100mg/L (W0). It revealed that the  
 5 peaks of the acicular and prismatic were increase after the impregnation in ferric  
 6 solution.



21 Fig. 2. SEM images (a:VA; b: FVA), XRD analysis (c) and pH<sub>pzc</sub> (d) of volcanic ash before and after  
 22 impregnation in ferric solution.

### 23 3.2. Batch adsorption study

#### 24 3.2.1. Determination of pH<sub>PZC</sub> and effect of solution pH on arsenic removal

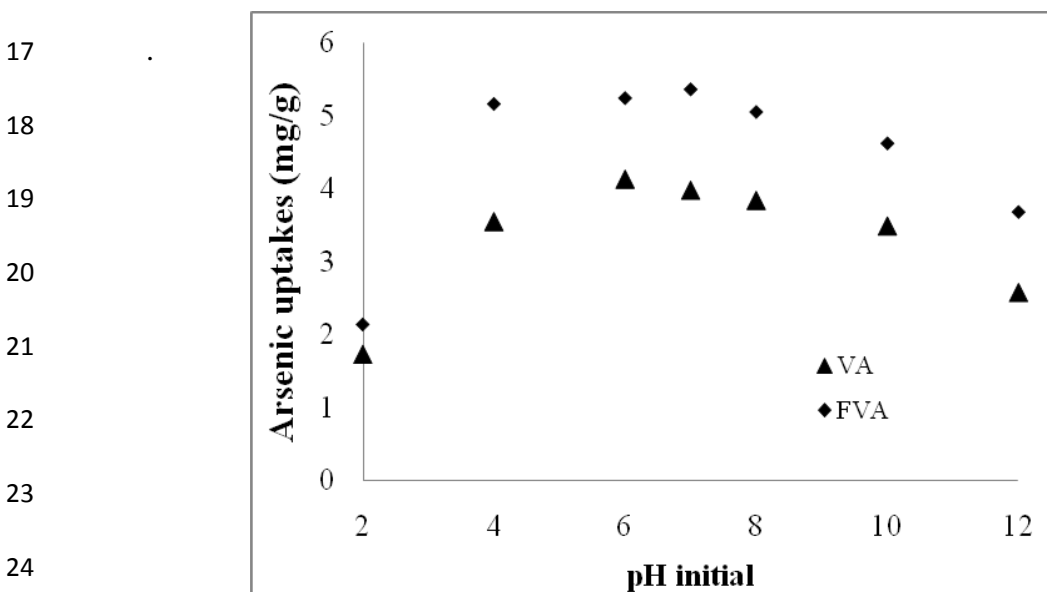
25 The pH value of solution where the net surface charge of adsorbent is zero is defined as pH<sub>PZC</sub>. As indicated in Fig. 2d, a plot of pH values of filtered solution after



1 equilibrium ( $\text{pH}_{\text{final}}$ ) as a function of initial pH values ( $\text{pH}_{\text{initial}}$ ) provides  $\text{pH}_{\text{PZC}}$  of the  
2 adsorbents by the common plateau of constant pH to the ordinate at around  $\sim 6.9$   
3 and  $\sim 5.5$  for VA and FVA, respectively. As a typical lewis acid,  $\text{FeCl}_3$  solution varied  
4 the sorbability of the electrolytes and degree of  $\text{H}^+$  and  $\text{OH}^-$  ions adsorption, and  
5 hence decrease the value of  $\text{pH}_{\text{PZC}}$  [21].

6 It is reported that adsorption anionic pollutant adsorption from aqueous medium  
7 depends heavily on the protonation pH range of the predominant metallic oxidic  
8 group, which affects the surface charge of the adsorbent particles and the ionization  
9 degree [22]. As indicated in Fig. 3, experiment data of arsenic adsorption on VA and  
10 FVA show a increase trend in As(V) removal efficiency with the declining of initial  
11 solution pH. It can be interpreted that the surface of adsorbents were partially  
12 positively charged at  $\text{pH} < \text{pH}_{\text{pzc}}$ , which provided more adsorption sites for the  
13 predominant arsenic species ( $\text{H}_2\text{AsO}_4^-$  or  $\text{HAsO}_4^{2-}$ ). The decrease of adsorption  
14 efficiency at  $\text{pH} < 4$  was probably due to the adsorbent loss caused by the  
15 solubilization and/or degradation.

### 16 3.2.2. Adsorption behavior on VA and FVA



25 Fig. 3. Effect of pH on As (V) adsorption by FVA, (initial As = 50mg/L; FVA dosage = 10 g /L; contact time = 48 h; T = 20°C).

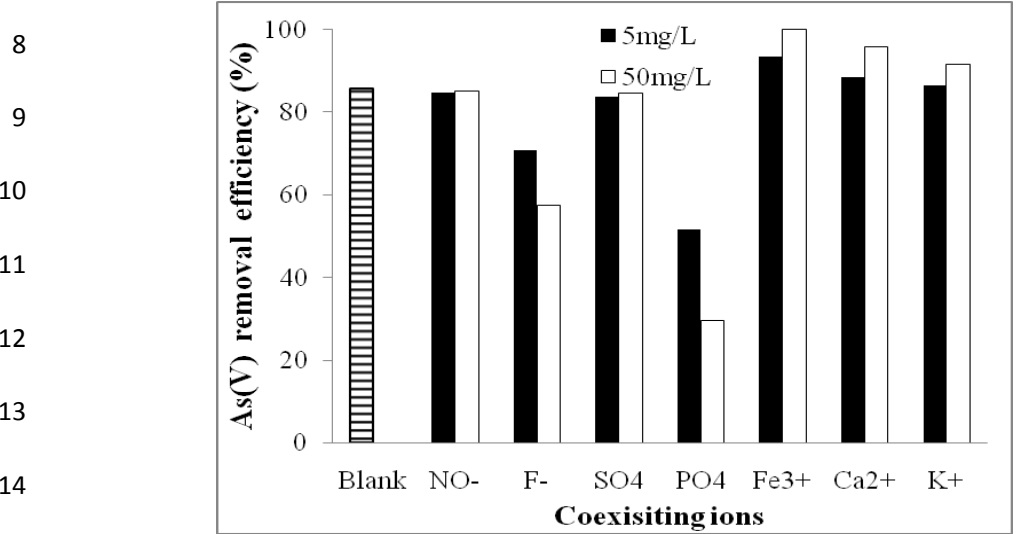
1           The experimental results (Fig. 3) show the iron impregnated onto volcanic ash  
2 greatly elevated the As (V) removal ability under all investigated pH condition.  
3 Recently, many previous studies focused on ferric based absorbents or ferric-arsenic  
4 co-precipitation for arsenic removal [16, 23]. However, in this study, the adsorption  
5 elevation may not only due to iron-arsenic co-precipitation caused by the formation of  
6 iron (hydro)oxides, but also due to the decline of  $pH_{PZC}$  resulting in a enhancement of  
7 electrostatic attraction at neutral pH.

### 8 *3.2.3. Effects of water mineralization*

9           The effects of water mineralization, mainly focused on the coexisting ions and  
10 ionic strength, on the arsenic removal efficiency was studied. The effect of coexisting  
11 ions on As(V) removal by FVA is presented in Fig. 4. The presence of sulfate and  
12 nitrate did not perceptibly interfere with As(V) removal even at the higher  
13 concentration of 50 mg/L (85.6% to 84.7% and 85.2%, respectively). However, both  
14 fluoride and phosphate exhibited obvious adverse effects on As(V) removal. The  
15 adsorption efficiency decreased quickly from 85.6% to 57.4% with an increase of  
16 fluoride concentration from 5 to 50 mg/L. The competitive ability of phosphate was  
17 much higher than that of fluoride, As(V) removal dramatically decreased from 85.6%  
18 to 29.6% with an increase of phosphate concentration from 5 to 50 mg/L. This  
19 phenomenon suggested that some adsorption sites on the surface of FVA can be  
20 occupied by the arsenate, phosphate and fluoride; and that the adsorption sites had a  
21 stronger effect on phosphate than on arsenate or fluoride. Sun et al. [18] reported that  
22 phosphate evidently inhibited arsenate removal due to competition between arsenate  
23 and phosphate species.

24           All of the investigated coexisting cations enhanced the As(V) removal ability on  
25 FVA (Fig. 4). The As(V) adsorption efficiency significantly elevated from 85.6% to

1 93.6% with the addition of 5 mg/L of  $\text{Fe}^{3+}$ . The univalent cation  $\text{K}^+$ , and  
 2 bivalent cation  $\text{Ca}^{2+}$  showed a similar trend but with an inferior effect compared with  
 3 trivalent cation  $\text{Fe}^{3+}$ . It can be stated that the ferric ion was prone to form  
 4 hydroxylated complex, like ferric hydroxide that can provide higher affinity to  $\text{As(V)}$ ,  
 5 thereby activate the adsorption ability of FVA. Zhang et al. [24] reported that metallic  
 6 cations can link the adsorbent particle with arsenate, forming a metal–arsenate  
 7 complex or a metal– $\text{H}_2\text{O}$ –arsenate complex.



15 Fig. 4. Effect of coexisting ions on  $\text{As(V)}$  adsorption: (initial  $\text{As} = 50 \text{ mg/L}$ ;  
 16 FVA dosage = 10 g/L; contact time = 24 h;  $T = 20^\circ\text{C}$ ; initial  $\text{pH} = 6.9$ ,  
 agitation speed = 200 rpm, the coexisting ions concentration: 5 and 50 mg/L.)

17 The ionic strength gave a slight effect on  $\text{As(V)}$  sorption with FVA (Table 3).  
 18 When the solution ionic strength was increased from 0.001 to 0.1M, the  $\text{As(V)}$  uptake  
 19 increased only from 5.35 to 5.82 mg/g. However, the obtained data were all higher  
 20 than that of a blank experiment with DI water. These trends were indicative of an  
 21 inner-sphere sorption mechanism for  $\text{As(V)}$ , which probably meant an exchange of  
 22 aqueous ligand for surface hydroxyl complexes might be generated on the surface of  
 23 inner-sphere. These trends are consistent with the results reported by Goldberg et al.  
 24 [25] and Fuller et al. [26], in which arsenate sorption onto mineral surfaces was due to  
 25 the formation of inner sphere complexes.

1 Table 3

2 Effect of solution ionic strength on As(V) adsorption by FVA

20°C	ionic strength			
Ionic strength	0	0.001M	0.01M	0.1M
As(V) Uptake (mg/g)	5.31	5.35	5.48	5.82
Electric Conductivity (us/cm)	< 1	138.8	1.24×10 <sup>3</sup>	12.57×10 <sup>3</sup>

3 Initial As = 50 mg/L; dosage = 10 g/L; contact time = 24 h; pH = 6.9, agitation speed = 200 rpm.

4

5 Fig.5 shows that As(V) adsorption efficiency with < 150 mesh FVA in DI water

6 at 35°C was 87.64% which is higher than that with < 150 mesh FVA at 20°C

7 (85.6%), > 14 mesh FVA at 35°C (77.54%) and > 14 meshes FVA at 20°C (75.21%).

8 However, the experiment performed under the conditions above in the actual water

9 sample (W1 and W2) showed a greatly elevated arsenic removal efficiency,

10 demonstrating that reaction between the  $\text{HAsO}_4^{2-}$  and the coexisting ions in actual

11 water sample can enhance the sorptive properties of FVA. The arsenic adsorption in

12 the higher mineralized water W2 resulted in the higher As(V) removal efficiency. It is

13 suggested that the water mineralization might be the key factor in determining the

14 As(V) adsorption performance comparing to the surface area of adsorbents and

15 adsorption temperature.

16

17

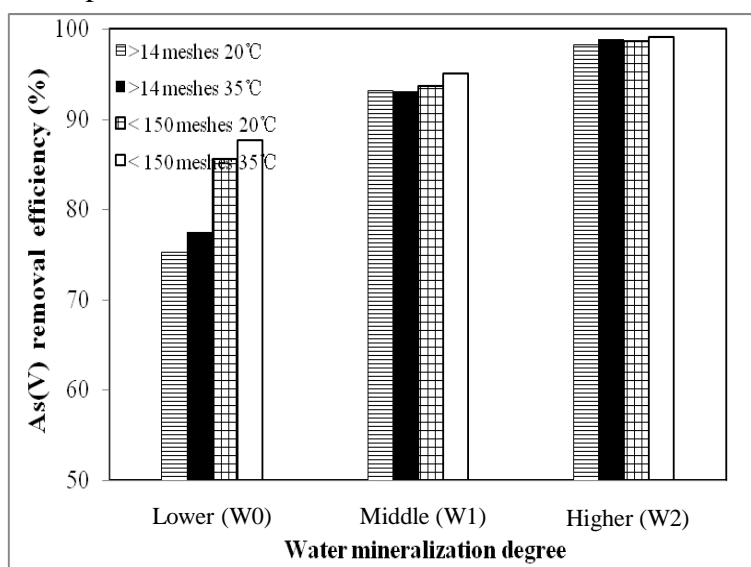
18

19

20

21

22



23

24 Fig. 5. Comparison effects of water mineralization, adsorption temperature  
25 and particle size of FVA on As (V) adsorption (initial As = 50 mg/L; FVA  
dosage = 10 g/L; initial pH = 6.9, agitation speed = 200 rpm)

25

All of the above results indicate that the mineralization of aqueous medium show

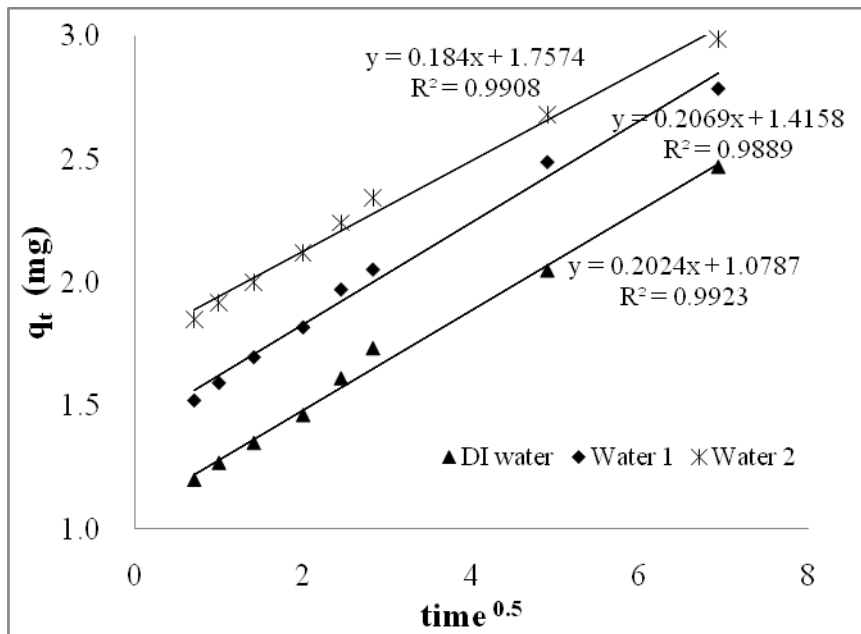
1 a marked effects on the arsenic adsorption. Therefore, it is important to investigate  
 2 arsenic removal based on actual waters rather than deionized water.

3 *3.2.4. Adsorption rate in different water samples*

4 Based on the research above, actual and DI water samples were applied in kinetic  
 5 study. In this experiment, the pseudo-first-order, pseudo-second-order, and  
 6 intraparticle diffusion models were used to discuss kinetic parameters of As(V)  
 7 adsorption on FVA. The experiment data showed As(V) adsorption  
 8 pseudo-equilibrium was achieved after approximately 48 h. Such a long adsorption  
 9 time probably indicated that adsorption could be due to not only the surface  
 10 adsorption on the particles but also chemisorption between the mineral matter and the  
 11  $\text{HAsO}_4^{2-}$  in actual water. The experiment data best fitted in intraparticle diffusion  
 12 equation:

13 
$$q_t = k_i t^{0.5} + C \quad (1)$$

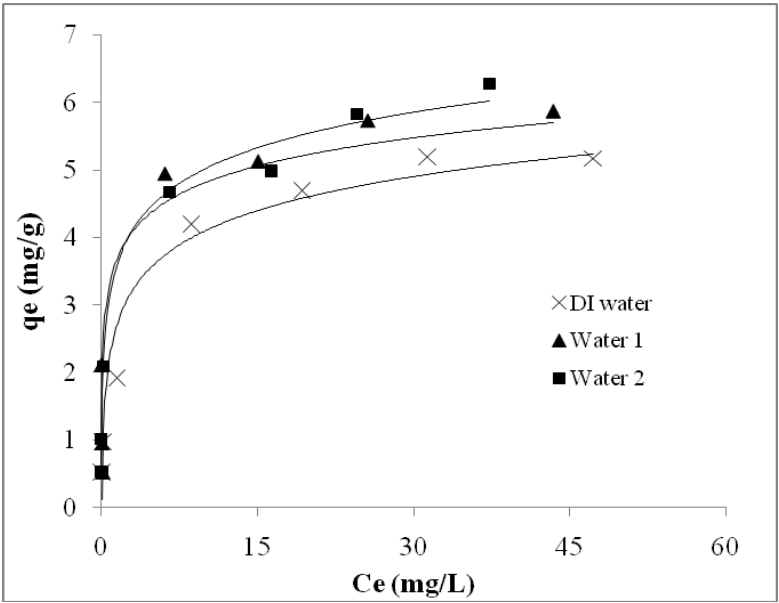
14 where  $q_t$  is the As(V) adsorption amount at time  $t$ ,  $k_i$  is the intra-particle diffusion rate  
 15 constant ( $\text{mg/g/h}^{-0.5}$ ) which can be calculated from the slopes of linear plot ( $q_t$  versus  $t$   
 16  $^{0.5}$ ) and  $C$  is the intercept depicting the boundary layer effect.



17  
18  
19  
20  
21  
22  
23  
24  
25  
 Fig. 6. Intraparticle diffusion plot for arsenic As (V) adsorption on FVA in different water samples (initial As= 10 mg/L; FVA dosage = 10 g/L; contact time = 48 h; T = 20 ± 0.5°C; initial pH = 6.9, agitation speed = 200 rpm).

1 The larger intercept from the higher initial concentration indicated that  
 2 chemisorption provides a greater contribution than surface adsorption, which was  
 3 probably due to the accompanying reaction caused by complex composition of the  
 4 nature adsorbent and actual water. As Ciardelli et al. [27] described the arsenic uptake  
 5 efficiency can be increased by coprecipitation with ferric oxyhydroxides and calcium  
 6 carbonate existed in the aqueous medium. Fig. 6 also shows that the plots do not pass  
 7 through the origin, which indicated the intraparticle diffusion was not only the rate  
 8 controlling step [28], and both the surface adsorption and intraparticle diffusion  
 9 contributed to the mechanism of arsenic adsorption.

10 *3.2.5. Isotherm study*



19 Fig. 7. Langmuir plots for As(V) adsorption on FVA in different water samples  
 20 (initial As: varied from 5 to 100 mg/L; FVA dosage = 10 g/L; contact time = 24  
 21 h; T = 20 ± 0.5°C; initial pH = 6.9, agitation speed = 200 rpm).

21 The As(V) adsorption were carried out in different water samples with an initial  
 22 arsenic concentration of 5, 10, 20, 50, and 100 mg/L (Fig. 7). The experiment data  
 23 from all water samples fitted the Langmuir isotherm well, which indicates that the  
 24 reaction is a reversible monolayer phenomenon [29] and the adsorbents have the  
 25 regeneration potential. The linearized forms of Langmuir isotherm equation is:

1  $1/q_e = (1/Q*b*C_e) + 1/Q,$  (2)

2 where  $q_e$  is the amount of solute adsorbed (mg/g) at equilibrium and  $C_e$  is the  
3 equilibrium concentration (mg/L), The values of the empirical constants  $Q$  and  $b$ ,  
4 denoting the monolayer capacity and energy of adsorption, were calculated from the  
5 slope and intercept of plot between  $C_e/q_e$  and  $C_e$ . Fig. 7 and Table 4 show that the  
6 As(V) adsorption on FVA in water sample W2 results in the highest removal capacity  
7 of 6.13 mg/g (estimated by Langmuir isotherm), followed by 5.92 mg/g in W1 and  
8 5.30 mg/g in W0. The experimental data is 5.98, 5.88 and 5.34 mg/g, respectively,  
9 which is in agreement with the calculated ones, further confirming that the adsorption  
10 on FVA well fit to Langmuir isotherm.

11 As the composition of water samples shown in Table 1, the mineralization  
12 degree is very low for water sample W0, while it is moderate for samples W1, being  
13 higher the concentrations of  $Na^+$ ,  $Ca^{2+}$ ,  $Cl^-$  and  $SO_4^{2-}$  in the latter. The water sample  
14 W2 is higher mineralized, with high contents of  $Na^+$ ,  $Ca^{2+}$ ,  $K^+$ ,  $Mg^{2+}$ ,  $Cl^-$ ,  $NO_3^-$  and  
15  $SO_4^{2-}$ . The mineralization degree increase through waters W0 to W2 (Table 1), and the  
16 general trend of the arsenic adsorption efficiency is to grow in the same way, that  
17 indicated the mineralization degree of water samples elevated the As(V) removal  
18 efficiency on FVA. This result can also be proved by the effect of coexisting ions on  
19 the As(V) removal researched above, the anions in the studied water samples mainly  
20 consisted of  $Cl^-$ ,  $NO_3^-$  and  $SO_4^{2-}$ , which evidently had no significant effect on the  
21 As(V) removal in the current concentrations limit. However, the dominated coexisting  
22 bivalence cations, such as  $Ca^{2+}$  and  $Mg^{2+}$ , enhanced the As(V) adsorption efficiency  
23 conclusively.

24

25

1 Table 4  
 2 Langmuir Isotherm parameters for As(V) adsorption on FVA in different water samples

Water sample	Langmuir constants		
	Correlation coefficient $r^2$ (%)	Q (mg/g)	b (L/ $\mu$ mol)
DI water	0.9973	5.3008	1.2811
Water 1	0.9977	5.9210	0.9822
Water 2	0.9894	6.1361	1.0554

3 Initial As: varied from 5 to 100 mg/L; dosage = 10 g/L; contact time = 24 h; T = 20  $\pm$  0.5°C; pH = 6.9,  
 4 agitation speed = 200 rpm.

5 It has been reported that the adsorption of As(V) by neutralized red mud [11],  
 6 hematite [17], and synthetic zeolites [20], follow Langmuir isotherm. The maximum  
 7 As(V) uptake, as estimated by Langmuir equation, of these adsorbents are 0.69, 0.20  
 8 and 34.8 mg/g, respectively. It is evident that FVA is more effective than neutralized  
 9 red mud and hematite. In this connection, synthetic zeolite seem to be more  
 10 advantageous adsorbents but the FVA is an attractive material in view of being  
 11 inexpensive and effect in a large pH range.

### 12 3.5. Possible mechanism of arsenic adsorption

13 Fig. 8a shows a SEM picture for the adsorbed FVA, and its corresponding  
 14 element mapping as revealed by EDX. It further confirms that FVA is primarily a  
 15 mixture of Si, Fe and Al oxides. Fig. 8 shows Si, Al and O evenly distributed on the  
 16 surface, iron is seen to be very well-dispersed all throughout the FVA (Fig. 8c).  
 17 Comparison with As mapping (Fig. 8d) suggests that iron is closely associated with  
 18 As, which implied that the As was bound with iron oxide. This suggests that the  
 19 amount of As adsorbed on the surface of FVA possibly depended on the iron content  
 20 of the particle surface.

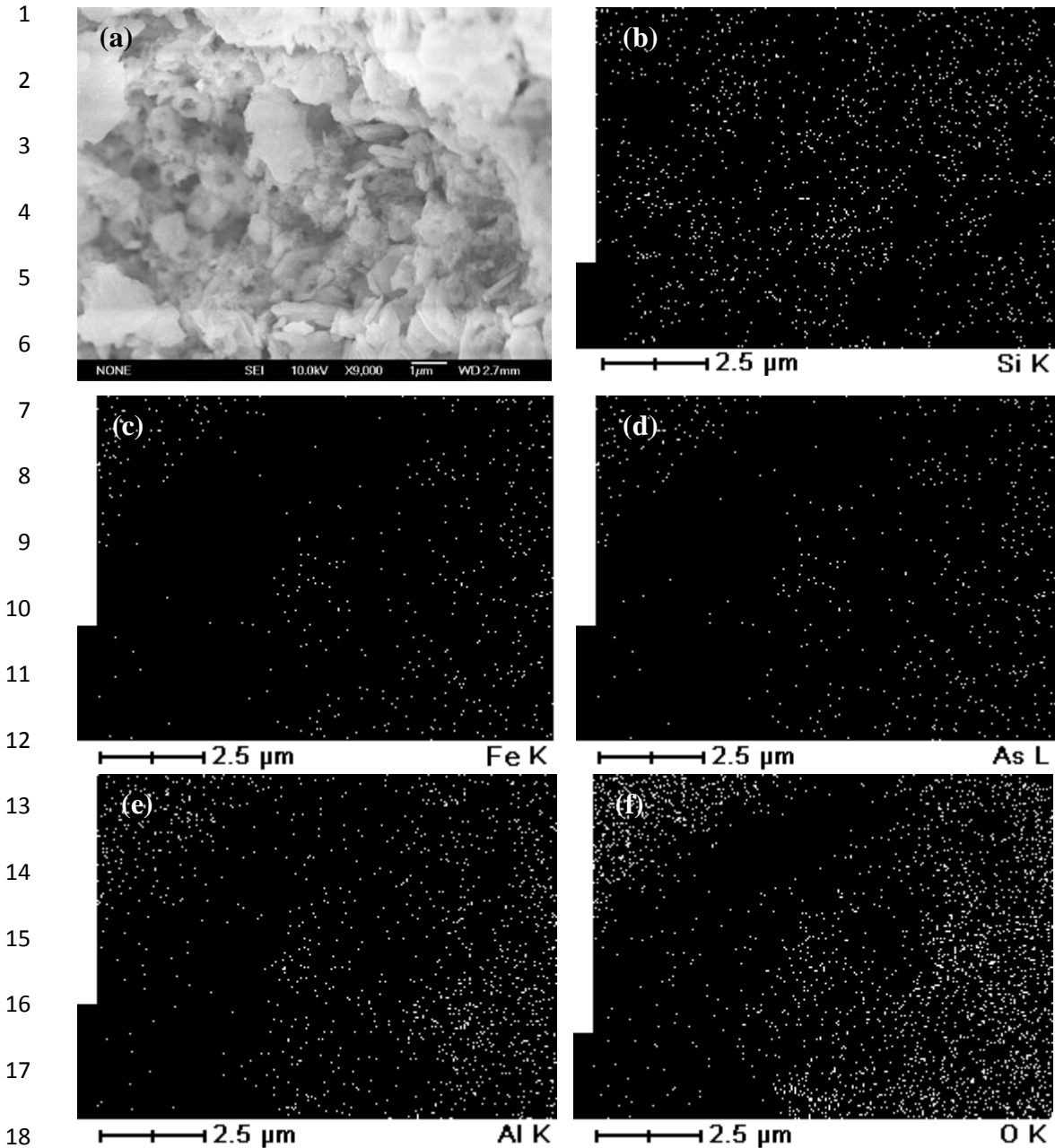
21

22

23

24

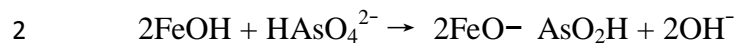
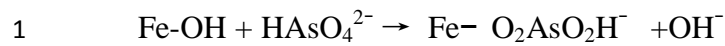




19 Fig.8. SEM images of adsorbed FVA (a), and mapping of elements: (b) Si, (c) Fe, (d) As, (e) Al and (f) O, as seen by EDX (energy dispersion of X-rays).

20 Based on the available data, the mechanism of As removal by FVA could not be  
 21 explained in full detail, though it is evident that it involves electrostatic attraction and  
 22 surface complexation processes between the As species in solution and Fe(II) and/or  
 23 Fe(III)-hydroxides in the solid materials. We assumed the possible mechanism as  
 24 below.





3 The adsorption of As(V) onto FVA occurred by ligand exchange reactions, and  
4 most of the hydroxide groups are involved in ligand exchange reactions. During the  
5 adsorption, the arsenate oxyanion present in the aqueous solution would replace the  
6 hydroxyl ions in the iron crystal lattice without disturbing the crystal structure of the  
7 compound. This type of substitution is iso-electronic in nature, as reported by  
8 Maliyekkal and Shukla [30]. The cumulative hydroxide group release per amount of  
9 arsenic adsorbed was related with amount of arsenic adsorbed [31]. The amount of  
10 goethite on the surface of FVA is proportional to the removal of arsenic. As shown in  
11 Fig. 7, the Langmuir Isotherm Model fits the experimental data well, because  
12 iron-hydroxide plays as an adsorption site for arsenic. The intraparticle diffusion  
13 analysis also indicated that chemisorption provides a greater contribution than surface  
14 adsorption, to the adsorption process.

#### 15 **4. Conclusions**

16 Ferric impregnated volcanic ash (FVA) is a cost-effective adsorbent for arsenic  
17 removal from water solution, especially from low-level phosphate and fluoride  
18 solution. The relationship between water mineralization degree and As(V) removal  
19 was attributed to the competitive or elevated effect of coexisting ions on FVA and  
20 ionic strength in the surrounding aqueous medium. The kinetic and isotherm studies  
21 conducted in actual water revealed that the mineralization of water showed great  
22 influence on the arsenic adsorption. It is suggested that the deionized batch  
23 experiment should not be applied directly to all cases. It was important to conduct the  
24 adsorption experiment using the actual water. Further research is underway to  
25 examine the adsorbent stability and whether the FVA can maintain its capability after

1 several regenerations and reuse cycles.

## 2 **Acknowledgements**

3 Chemical and micromorphology analyses of FVA were carried out at National  
4 Institute for Materials Science (NIMS), Tsukuba, Japan, The authors wish to express  
5 their thanks to Dr. Zhi Chunyi.

## 6 **References**

- 7 [1] WHO. Arsenic. Environmental Health Criteria 18, IPCS International Programme  
8 of Chemical Safety. Vammala (Finland): Vammalan Kõirjapaino Oy., 1981.
- 9 [2] H. Brammer., P. Ravenscroft, Environ. Int. 35 (2009) 647–654.
- 10 [3] R.T Nickson, J.M. McArthur, P. Ravenscroft, W.G. Burgess, K.M. Ahmed, Appl  
11 Geochem. 15 (2000) 403–413.
- 12 [4] H.M. Guo, Y.X. Wang, G.M. Shpeizer, S. Yan, J. Environ. Sci. Health A 38 (2003)  
13 2565–2580.
- 14 [5] WHO, Guidelines for Drinking-water Quality, Health Criteria and Other  
15 Supporting Information, vol. 2. World Health Organization, Geneva, 1996.
- 16 [6] EC, Directive related with drinking water quality intended for human consumption,  
17 European Commission, Brussels, 1998.
- 18 [7] EPA, Implementation guidance for the arsenic rule, EPA Office of Groundwater  
19 and Drinking Water, Cincinnati, 2002.
- 20 [8] G.L. Ghurye, D.L. Clifford, A.R. Tripp, J. Am. Water Works Assoc. 91 (1999)  
21 85–96.
- 22 [9] H. Garelick, A. Dybowska, E. Valsami-Jones, N.D. Priest, J. Soils Sediments. 5  
23 (2005) 182–190.
- 24 [10] P. Mondal, C.B. Majumder, B. Mohanty, J. Hazard. Mater. B137 (2006) 464–479.
- 25 [11] H. Genc-Fuhrman, J.C. Tjell, D. McConchie, J. Colloid Interface Sci. 271 (2004)

- 1 313–320.
- 2 [12] A.F. Bertocchi, M. Ghiani, R. Peretti and A. Zucca, *J. Hazard. Mater.* B134  
3 (2006) 112–119.
- 4 [13] P. Webley, L. Mastin, *J. Volcanol. Geoth. Res.* 186 (1-2) (2009) 1-9.
- 5 [14] Y.H. Xu, T. Nakajima, A. Ohki, *J. Hazard. Mater.* B 92 (2002) 275–287.
- 6 [15] S.W. Al Rmalli, C.F. Harrington, M. Ayub, P.I. Haris, *J. Environ. Monit.* 7 (2005)  
7 279–282.
- 8 [16] S. Bang, G.P. Korfiatis, X.G. Meng, *J. Hazard. Mater.* 121 (2005) 61–67.
- 9 [17] H.M. Guo, D. Stuben, Z. Berner, *Appl Geochem.* 22 (2007) 1039–1051.
- 10 [18] H.W. Sun, L. Wang, R.H. Zhang, J.C. Sui, G.N. Xu, *J. Hazard. Mater.* B129  
11 (2006) 297–303.
- 12 [19] L.C. Roberts, S.J. Hug, T. Ruettimann, *Environ. Sci. Technol.* 38 (2004)  
13 307–315.
- 14 [20] P. Chutia, S. Kato, T. Kojima, S. Satokawa, *J. Hazard. Mater.* 162 (2009)  
15 440–447.
- 16 [21] D. Borah, K. Senapati, *Fuel.* 85 (2006) 1929–1934.
- 17 [22] I.D. Smiciklas, S.K. Milonjic, P. Pfendt, S. Raicevic, *Sep. Purif. Technol.* 18  
18 (2000) 185–194.
- 19 [23] J. Hlavay, K. Polyak, *J. Colloid Interface Sci.* 284 (2005) 71–77.
- 20 [24] S.W. Zhang, C.J. Liu, Z.K. Luan, X.J. Peng, H.J. Ren, J. Wang, *J. Hazard. Mater.*  
21 152 (2008) 486–492.
- 22 [25] S. Goldberg, C.T. Johnston, *J. Colloid Interface Sci.* 234 (1) (2001) 204–216.
- 23 [26] C.C. Fuller, J.A. Davis, G.A. Waychunas, *Geochim. Cosmochim. Acta.* 57 (10)  
24 (1993) 2271–2282.
- 25 [27] M.C. Ciardelli, H.F. Xu, N.Sahai, *Water Res.* 42 (2008) 615 – 624.

- 1 [28] V.K. Gupta, V.K. Saini, N. Jain, J. Colloid Interface Sci. 288 (2005) 55–60.
- 2 [29] K.S. Gupta, K.Y. Chen, J. WPCF. 50 (1978) 493–499.
- 3 [30] S.M. Maliyekkal, S. Shukla, L. Philip, I.M. Nambi, J. Chem. Eng. 140 (2008)
- 4 183–192.
- 5 [31] A. Jain, K.P. Raven, R.H. Loepfert, Environ. Sci. Technol. 33 (1999) 1179–1184.